Constrained molecular dynamics approach to fermionic systems

Massimo Papa,[1,2,*] Toshiki Maruyama,[1,3,†] and Aldo Bonasera[1,‡]
[1]*Istituto Nazionale Fisica Nucleare-Laboratorio Nazionale del Sud, Via Santa Sofia 44, I-95123 Catania, Italy*
[2]*Istituto Nazionale Fisica Nucleare-Sezione di Catania, Corso Italia 57, I-95129 Catania, Italy*
[3]*Advanced Science Research Center, Japan Atomic Energy Research Institute, Shirakata Shirane 2-4, Tokai, Naka Ibaraki 319-1195, Japan*
(Received 19 December 2000; published 13 July 2001)

We propose a constrained molecular dynamics model for a fermionic system. In this approach the equations of motion of the centroids related to the single-particle phase-space distributions are solved by imposing that the one-body occupation probability $\overline{f_i}$, evaluated for each particle, can assume only values less than or equal to 1. This condition reflects the fermionic nature of the studied systems, and it is implemented with a fast algorithm which allows also the study of the heaviest colliding system. The parameters of the model have been chosen to reproduce the average binding energy and radii of nuclei in the mass region $A=30-208$. Some comparison to the data is given.

DOI: 10.1103/PhysRevC.64.024612 PACS number(s): 25.70.−z, 21.10.Dr, 24.10.Lx, 24.60.−k

I. INTRODUCTION

Heavy ion collisions in the medium-energy region have been described in a large variety of semiclassical approaches to the many-body problem. As is well known the one-body semiclassical transport models like the Boltzmann-Nordheim-Vlasov (BNV) [1] and Vlasov-Uehling-Uhlenbeck (VUU) [2] models are not suited to describe processes in which a large number of final fragments are produced. This is due to the fact that the correlations treated in the one-body approach are not able to describe the large fluctuations which develop in a multifragmentation process.

This difficulty can be solved by adopting more suitable treatments of the *N*-body problem like molecular dynamics. Several molecular dynamics models have been developed up to now [3]. In the quantum molecular dynamics (QMD) [4] model the *N*-body wave function is expressed through a direct product of wave packets, each of which satisfies the minimum uncertainty relation $\sigma_r\sigma_p=\hbar/2$, where σ_r and σ_p represent the dispersion of the corresponding Wigner transform in configuration and momentum space, respectively.

The fermionic nature of the nuclear many-body problem has been considered in the fermionic molecular dynamics [5,6] model and more recently in the antisymmetrized molecular dynamics (AMD) [6,7] model. In these models, the wave function of the system is expressed as a single Slater determinant of *N* wave packets. In this way the fermionic nature of the system is preserved. In particular in the AMD approach two-body collisions are introduced in the ''physical coordinates'' which are obtained by a canonical transformation from the parameter coordinates of wave packets [7]. The nucleon-nucleon collision is only allowed when an inverse transformation from a newly chosen ''physical coordinate'' (the final state of the collision) into the corresponding parameter coordinate exists. This condition is understood as a stochastic change of state from a single Slater determinant into another. As a result of the four-dimensional matrix element of the two-body interaction, the CPU time necessary to work out calculations for systems with total mass larger than 200 is very large for practical studies.

On the other hand, the QMD calculations are much easier to carry out because they need in general only double-fold loops to calculate two-body interactions. But it is obvious that the fermionic feature is lacking in the QMD model. Two-body collisions are also introduced phenomenologically. The Pauli blocking of the final state is usually checked in a similar manner to the collision term in the BNV model. The two-body collisions with Pauli blocking have some effects to maintain the fermionic feature of the system. However, in the ground states or in low-energy reaction phenomena, two-body collisions are absent or very rare. Even if the initial state is in agreement with the phase-space distribution of a fermionic system, the time evolution by classical equations of motion surely breaks the initial distribution which evolves into a classical Boltzmann one.

To compensate this shortcoming, the Pauli potential is introduced by several authors to mimic the fermionic features [8–10]. This phenomenological potential forbids nucleons of the same spin and isospin from coming close to each other in phase space. Although the Pauli potential gives some good results such as stable ground states, with energies in agreement with experiments and saturation properties of nuclear matter, it also gave some undesirable byproducts: for instance, spurious repulsion in the collision problem.

In the present work we propose a new molecular dynamics model: the constrained molecular dynamics (CoMD) model, which aims to overcome the above-mentioned limitations. In particular we want

(i) to describe the fermionic nature of the *N*-body system with the more general condition that the occupation probability $\overline{f}\leqslant 1$ and

(ii) to realize a model for which the computational time is short enough to allow the study of the heaviest systems.

*Electronic address: papa@lns.infn.it
†Electronic address: maru@hadron02.tokai.jaeri.go.jp
‡Electronic address: bonasera@lns.infn.it

II. MODEL

A. Theoretical framework

In QMD, each nucleon state is represented by a Gaussian wave function of width σ_r,

$$\phi_i(\mathbf{r}) = \frac{1}{(2\pi\sigma_r^2)^{3/4}} \exp\left[-\frac{(\mathbf{r}-\langle \mathbf{r}_i \rangle)^2}{4\sigma_r^2} + \frac{i}{\hbar}\mathbf{r}\cdot\langle \mathbf{p}_i \rangle \right], \quad (1)$$

where $\langle \mathbf{r}_i \rangle$ and $\langle \mathbf{p}_i \rangle$ are the centers of position and momentum of ith nucleon, respectively. The total wave function is assumed to be a direct product of these wave functions. Similarly the N-body distribution function is a direct product of the single-particle distribution functions f_i. The f_i are obtained by the Wigner transform of the wave functions ϕ_i and we can express the one-body distribution function $f(\mathbf{r},\mathbf{p})$ as

$$f(\mathbf{r},\mathbf{p}) = \sum_i f_i(\mathbf{r},\mathbf{p}), \quad (2)$$

$$f_i(\mathbf{r},\mathbf{p}) = \frac{1}{\pi^3\hbar^3} \exp\left[-\frac{(\mathbf{r}-\langle \mathbf{r}_i \rangle)^2}{2\sigma_r^2} - \frac{2\sigma_r^2(\mathbf{p}-\langle \mathbf{p}_i \rangle)^2}{\hbar^2} \right]. \quad (3)$$

We note that since σ_r is a real number in the QMD approach, the distribution function f_i produces the minimum uncertainty relation $\sigma_r\sigma_p = \hbar/2$ in one-body phase space.

In this paper we take the dispersion in momentum σ_p as a parameter as well as that in coordinate space. Therefore we write the distribution function of each nucleon as

$$f_i(\mathbf{r},\mathbf{p}) = \frac{1}{(2\pi\sigma_r\sigma_p)^3} \cdot \exp\left[-\frac{(\mathbf{r}-\langle \mathbf{r}_i \rangle)^2}{2\sigma_r^2} - \frac{(\mathbf{p}-\langle \mathbf{p}_i \rangle)^2}{2\sigma_p^2} \right]. \quad (4)$$

This distribution function can be in principle interpreted as a generalization of the exact classical one $f_i(\mathbf{r},\mathbf{p}) = \delta(\mathbf{r} - \langle \mathbf{r}_i \rangle)\,\delta(\mathbf{p} - \langle \mathbf{p}_i \rangle)$ describing pointlike particles.

The $f_i(\mathbf{r},\mathbf{p})$ and $f(\mathbf{r},\mathbf{p})$ are the physical quantities of interest from which we calculate all the relevant observables, such as densities, energies, mass distributions, etc. In this respect we could write $f(\mathbf{r},\mathbf{p})$ as a sum of other functions, such as triangular or theta functions. The use of Gaussians allows us to have simple differentiable expressions. The use of free parameters $\sigma_{r,p}$ helps in easily reproducing the basic ground state properties of nuclei, i.e., binding energies, radii, and Fermi motion of the nucleons.

The equations of motion of $\langle \mathbf{r}_i \rangle$ and $\langle \mathbf{p}_i \rangle$ are derived using the time-dependent variational principle which gives

$$\langle \dot{\mathbf{r}}_i \rangle = \frac{\partial H}{\partial \langle \mathbf{p}_i \rangle}, \quad \langle \dot{\mathbf{p}}_i \rangle = -\frac{\partial H}{\partial \langle \mathbf{r}_i \rangle}. \quad (5)$$

In our approach the total energy H for A particles with mass m consists of the kinetic energy and the effective interactions:

$$H = \sum_i \frac{\langle \mathbf{p}_i \rangle^2}{2m} + A\frac{3\sigma_p^2}{2m} + V. \quad (6)$$

The second term arises from the Gaussian width in p space. However, in the following considerations we omit such a constant term. This is a crucial assumption. In fact, if one keeps such a term in Eq. (6) and tries to reproduce the right binding energies, part (or all) of the Fermi motion will come from it. In particular when $3\sigma_p^2/2m \simeq 20$ MeV, the particle will be essentially at rest; i.e., the system will correspond to a solid.

B. Effective interaction

In this preliminary work we use a simple local Skyrme parametrization with a 200 MeV incompressibility as described in many review articles [1–6]. The symmetry term is also included. We recall in an explicit way an expression of several terms:

$$V = V^{\mathrm{vol}} + V^{(3)} + V^{\mathrm{sym}} + V^{\mathrm{surf}} + V^{\mathrm{Coul}}. \quad (7)$$

By defining the superimposition integral ρ_{ij} as

$$\rho_{ij} \equiv \int d^3r_i d^3r_j \rho_i(\mathbf{r}_i)\rho_j(\mathbf{r}_j)\,\delta(\mathbf{r}_i - \mathbf{r}_j), \quad (8)$$

$$\rho_i \equiv \int d^3p\, f_i(\mathbf{r},\mathbf{p}), \quad (9)$$

the terms in Eq. (7) can be written as

$$V^{\mathrm{vol}} = \frac{t_0}{2\rho_0} \sum_{i,j\neq i} \rho_{ij}, \quad (10)$$

$$V^{(3)} = \frac{t_3}{(\mu+1)(\rho_0)^\mu} \sum_{i,j\neq i} \rho_{ij}^\mu, \quad (11)$$

$$V^{\mathrm{sym}} = \frac{a_{\mathrm{sym}}}{2\rho_0} \sum_{i,j\neq i} [2\delta_{\tau_i,\tau_j} - 1]\rho_{ij}, \quad (12)$$

$$V^{\mathrm{surf}} = \frac{C_s}{2\rho_0} \sum_{i,j\neq i} \nabla^2_{\langle \mathbf{r}_i \rangle}(\rho_{ij}), \quad (13)$$

$$V^{\mathrm{Coul}} = \frac{1}{2} \sum_{\substack{i,j\neq i \\ (i,j\in \text{protons})}} \frac{e^2}{|\langle \mathbf{r}_i \rangle - \langle \mathbf{r}_j \rangle|} \mathrm{erf}\left(\frac{|\langle \mathbf{r}_i \rangle - \langle \mathbf{r}_j \rangle|}{2\sigma_r^2} \right). \quad (14)$$

In the above relations τ_i indicates the isospin degree of freedom and μ has been fixed to 7/6. The V^{vol} and the $V^{(3)}$ terms represent the two-body and the so-called three-body (or density-dependent) contributions. The values of t_0 and t_3 have been fixed to -356 MeV and 303 MeV. These values reproduce the saturation density ρ_0 and binding energy for symmetric nuclear matter with a compressibility of 200 MeV. The third term represents the symmetry term with $a_{\mathrm{sym}} = 32$ MeV.

Of particular importance is the surface $V^{\rm surf}$. We do not use the canonical value $C_s=-22.77$ MeV fm^2 [1–3,6], since a large part of the surface energy comes from $V^{\rm vol}$ and $V^{(3)}$ by using the Gaussian distribution function. Thus we leave C_s as a free parameter to reproduce the nuclear radii.

C. Numerical methods and the constraint

The set of equations expressed in Eq. (5) has been solved using a fourth-order Runge-Kutta method coupled with two numerical algorithms which aim to take into account the effects of the residual interaction and the fermionic nature of the many-body problem we are studying.

One consists of the usual two-body elastic collisions which mimic the effect of the short-range repulsive residual interaction together with the stochastic change of the phase-space distribution with Pauli blocking in the final states. The isospin-dependent parametrization of the nucleon-nucleon elastic angular distribution together with the concept of the mean free path has been used to compute the collision probability per unit of time [1]. The Pauli blocking factor, which is related to the constraint, is discussed later.

The other algorithm constraints at each time step the following quantities:

$$\overline{f_i} \leqslant 1 \quad (\text{for all } i), \tag{15}$$

$$\overline{f_i} \equiv \sum_j \delta_{\tau_i,\tau_j}\delta_{s_i,s_j}\int_{h^3} f_j(\mathbf{r},\mathbf{p})d^3r d^3p. \tag{16}$$

The coordinate s_i represents the nucleon spin projection quantum number. The integration is performed on an hypercube of volume h^3 in the phase space centered around the point $(\langle \mathbf{r}_i\rangle,\langle \mathbf{p}_i\rangle)$ with size $\sqrt{2\pi\hbar\sigma_r/\sigma_p}$ and $\sqrt{2\pi\hbar\sigma_p/\sigma_r}$ in r and p spaces, respectively. The quantities $\overline{f_i}$ can therefore be interpreted like an occupation density of the one-body phase space around the point of coordinate $(\langle \mathbf{r}_i\rangle,\langle \mathbf{p}_i\rangle)$. In general more than 60% of the occupation $\overline{f_i}$ arises from the contribution f_i of the particle i itself. Of course such a value depends strongly on the choices of $\sigma_{r,p}$. To realize the constraint expressed through the relation (15) the following procedure has been used.

At each time step and for each particle i an ensemble K_i of nearest identical particles (including the particle i) is determined within the distances $3\sigma_r$ and $3\sigma_p$ in the phase space. If the phase space occupation $\overline{f_i}$ has a value greater than 1, we change randomly the momenta of the particles belonging to the ensemble K_i in such a way that for the newly generated sample the total momentum and the total kinetic energy is conserved (''many-body elastic scattering''). The new sample is accepted only if it reduces the phase-space occupation $\overline{f_i}$. The most general way to generate these new samples is to change the momenta of all particles in K_i at a time. However, to reduce considerably the CPU time to generate new samples, we change, for each attempt, only the momenta of the particle i (the particle which gives the largest contribution to $\overline{f_i}$) and of a particle j in K_i. In this way the many-body scattering has been restricted to a series of two-body scatterings. A sufficiently small time step ensures that the constraint is reasonably realized as we will show in some numerical examples below (see Fig. 2).

To handle the Pauli blocking in the collision term is straightforward from the constraint. In fact for each NN collision we evaluate the occupation probability [see Eqs. (15) and (16)] after the elastic scattering. If such functions are both less than 1, the collision is accepted, and rejected otherwise. We notice that this procedure, dictated by the molecular dynamics approach, is in the same spirit as in AMD [7] where the collision is accepted if the final state is again a Slater determinant.

Finally we stress that the constraint acts in a way complementary to the collision term. In fact particles of low momenta are strongly effected by the constraint in such a way to avoid the distribution becoming a classical one. On the contrary the collision term is especially important for particles located at high relative momenta.

III. CALCULATIONS AND COMPARISON WITH OTHER MODELS

As an example we compare our results on the isotope distribution in ^{40}Ca+^{40}Ca at 35 MeV/nucleon with the experiment [11] and to the result of QMD. Finally we compare CoMD results to experimental data on central Au+Au collisions [12].

A. Initialization

The ground state configuration of a nucleus is obtained by using a modified cooling procedure. The nucleons are first distributed in a sphere of radius $1.4\times A^{1/3}$ fm in configuration space and in a sphere of radius $P_F^{\rm nm}$ (Fermi momentum for infinite nuclear matter) in momentum space. The equations of motion with friction terms are solved coupled with the constraint. At each time step, if the value of $\overline{f_i}$ is greater than 1, the momenta of the particles belonging to the ensemble K_i are scaled by a factor of 1.02. If $\overline{f_i}$ is less than 1, the scale factor is set to 0.98. With this procedure the total energy and the radius R of the nuclei will reach some stationary values. If the deviations of these values from the experimental ones are within 7%, a check is done on the stability. At this stage the friction term for the ''cooling'' is switched off and the time dependence of the nuclear radius R is checked. If R is stable at least for 1000 fm/c, this initial condition is accepted. In Fig. 1 we show R as a function of time for two typical ''good events'' representing the ^{40}Ca and ^{208}Pb nuclei. The binding energies are -8.2 and -8.4 MeV, respectively. The reason of the stability in the CoMD is the constraint. In fact, without the constraint, the initial fermionic distribution will evolve into a classical one. This means that during the interaction several particles will tend to have low relative momenta trying to reach a stable classical configuration (a classical ground state would be a solid) while some other particles (due to energy conservation) will acquire momenta large enough to overcome the

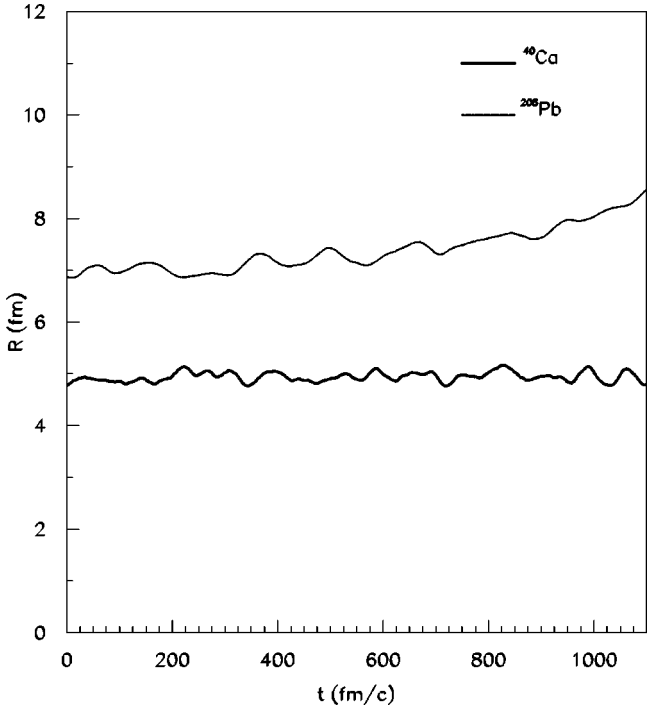

FIG. 1. Nuclear radii R as function of time for typical ground state configurations of ^{40}Ca and ^{208}Pb nuclei.

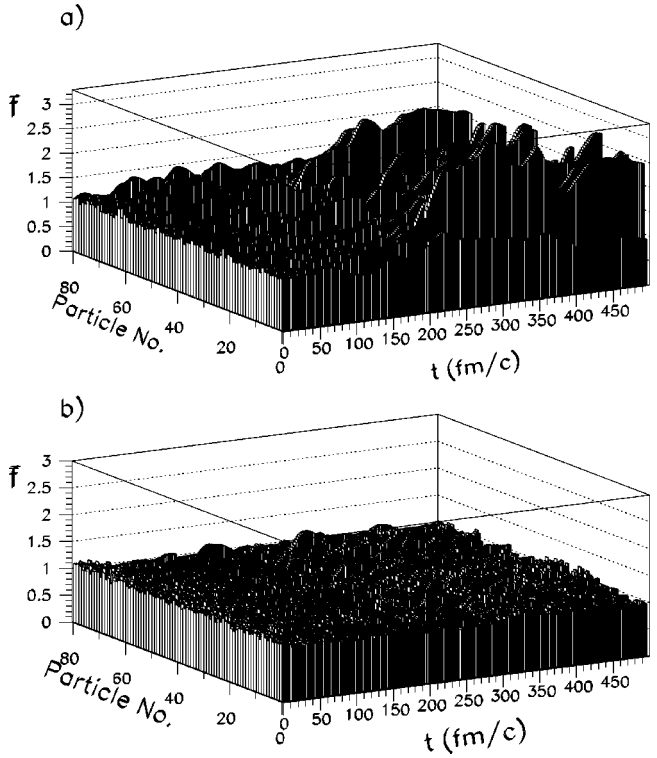

FIG. 2. Two-dimensional histograms showing the occupation probability $\overline{f_i}$ as a function of the particle index i and time for the system under study. The upper panel refers to the QMD case while the lower one is relative to the CoMD model.

barrier and leave the system. This does not happen in CoMD since the constraint maintains the fermionic nature of the system.

The results shown in Fig. 1 are obtained by setting $\sigma_r = 1.3$ fm, $\sigma_p/\hbar = 0.47$ fm^{-1}, and $C_s = -0.33$ MeV fm^2. The value of the surface term might be surprising at first, but we must notice that part of the surface term comes automatically when using a Gaussian. We observe also that using this procedure with the above set of parameters the effective average kinetic energy per nucleon, K (the kinetic energy regarding the centroid of the Gaussian distribution functions), is very close to the value obtained in a Thomas-Fermi model (about 20 MeV). This feature is instead lost in most of the molecular dynamics models while it is a peculiarity of the proposed one.

In fact in the present approach for a fixed average density and effective interaction, the ratio between the kinetic energy and potential one depends on σ_p. In particular we have verified that for a small increase of σ_p with respect to the value $\hbar/(2\sigma_r)$ the filling and especially the uniformity of phase space increase as a result of the larger overlap of the distribution function tails. This fact helps, during the cooling procedure, to maintain a relatively high value of the effective total kinetic energy (near the one that can be deduced from the Thomas-Fermi model) and to obtain more stable initial configurations.

Therefore we are able, in the global fit procedure, to find a set of parameters which reproduce the nuclear binding energies, the radii, and the ratio between K and the potential energy close to the value of the Thomas-Fermi model.

B. Nucleus-nucleus collision

In this section we show some results concerning the ^{40}Ca+^{40}Ca collision at $E_{\rm lab} = 35$ MeV/nucleon. In Fig. 2 we display the time dependence of $\overline{f_i}$ for all particle indices i in a typical event with zero impact parameter. The upper and lower parts show the results of the QMD and CoMD models, respectively, with exactly the same initial condition. The difference between the two cases is quite clear. In the QMD case after a short time (about 50 fm/c) the values of $\overline{f_i}$ for most of the particles start to be greater than 1 and are larger than 2 after some hundreds of fm/c. This result is easily understood. In the QMD case, which has no constraint regarding the fermionic nature except for the two-nucleon collision process, the momentum distribution tends to the classical limit. Obviously in the CoMD case, due to the constraint, the phase-space occupation $\overline{f_i}$ is on the average less than 1 at each time step. We note a good uniformity of $\overline{f_i}$ as a function of the particle index i and time t. These results obviously affect the collision rate r_c.

In Fig. 3 we show r_c as a function of t for central collisions for both the QMD and CoMD models. In the QMD case the collision rate steeply increases and decreases around 40 fm/c. This behavior can be explained as follows: although we use the same initial condition as the CoMD model, there appears some fluctuation of the occupation number $\overline{f_i}$ due to the classical nature of the QMD model. Therefore two-nucleon collisions are easier to occur at the beginning compared to the CoMD model. After about 30 fm/c, however, when the two nuclei start to overlap, $\overline{f_i}$ increases spuriously above 1. This causes a rapid decrease of

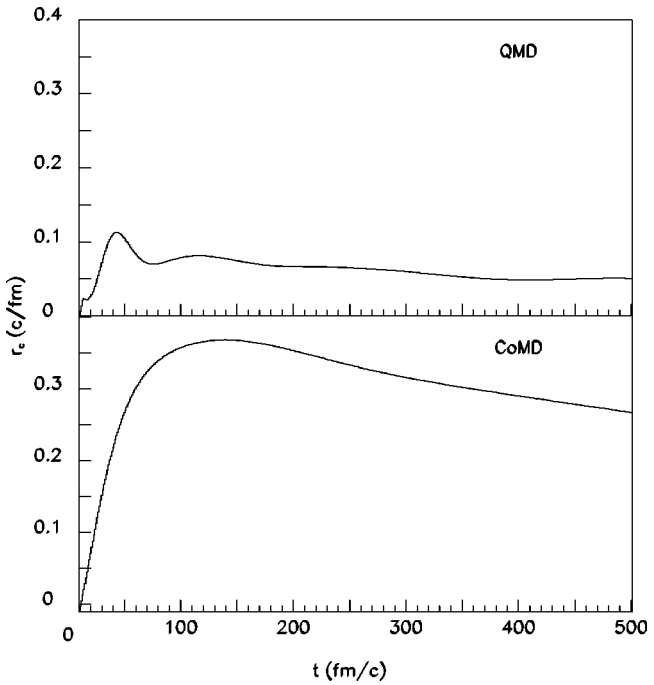

FIG. 3. Collision rate r_c as a function of time for the central collision ^{40}Ca+^{40}Ca at 35 MeV/nucleon in the QMD and CoMD cases.

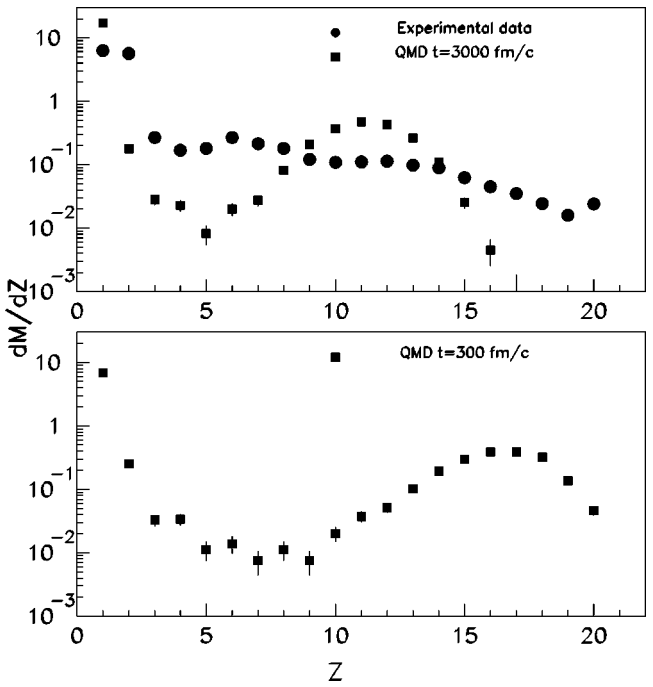

FIG. 4. Comparison between the experimental isotope distribution measured for the ^{40}Ca+^{40}Ca at 35 MeV/nucleon [11] system and the theoretical prediction performed according to the QMD approach. The calculations are shown at two different time intervals as indicated in the figure.

the collision rate in QMD calculations because of Pauli blocking. The behavior is completely different in the CoMD case. The collision rate develops in about 200 fm/c and reaches a value about 3 times greater than the maximum value relative to the QMD case, producing in turn more stopping. After this time the disassembled system, i.e., the fragments, gradually approaches its ground state, which causes a decrease of the collision rate. One may notice, however, a large collision rate even after several hundreds of fm/c. The reason for this large number is due to collisions with very low relative momenta which on the other hand have no effect on the dynamics.

In Figs. 4 and 5 we compare the isotope distribution given by the QMD and CoMD approaches with the experimental data on ^{40}Ca+^{40}Ca [11]. About 2000 events have been generated for an impact parameter range $b=0-8$ fm. The minimum spanning tree method [3] in configuration space has been applied to determine the fragments at $t=300$ fm/c and at $t=3000$ fm/c. We have verified that within the time 3000 fm/c all the fragments are stable. What we can also see from the figure is that the main features of the fragment mass distribution are already determined at 300 fm/c. After that the process is dominated by the emission of particles from the heavier fragments.

In the upper panel of Fig. 4 we compare the experimental isotope distribution to QMD at 3000 fm/c. We observe a clear disagreement between the QMD calculation and the experiment. The calculation shows essentially the binary character of the reaction while the experimental data show a significant production of the intermediate-mass fragment (IMF, $Z\geqslant 3$). The binary behavior shows some kind of transparency in the calculation. This transparency is caused by the lack of two-body collisions due to the overcrowding of the phase space as discussed above. At the bottom of Fig. 4 the result at 300 fm/c is shown. In this case we observe a similar behavior as above, the only difference being a shift of the main bump towards a higher value of Z and a more pronounced ''U'' shape. In Fig. 5 the same comparisons are

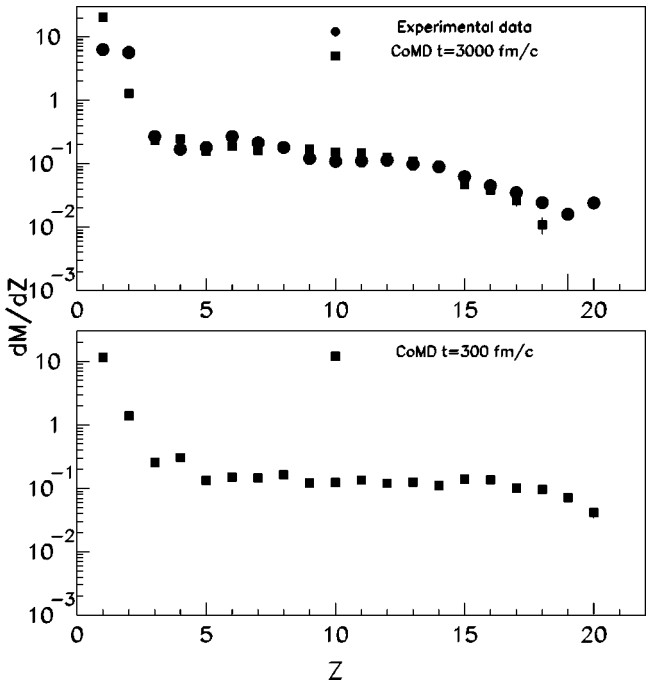

FIG. 5. Same as Fig. 4 but for the CoMD model.

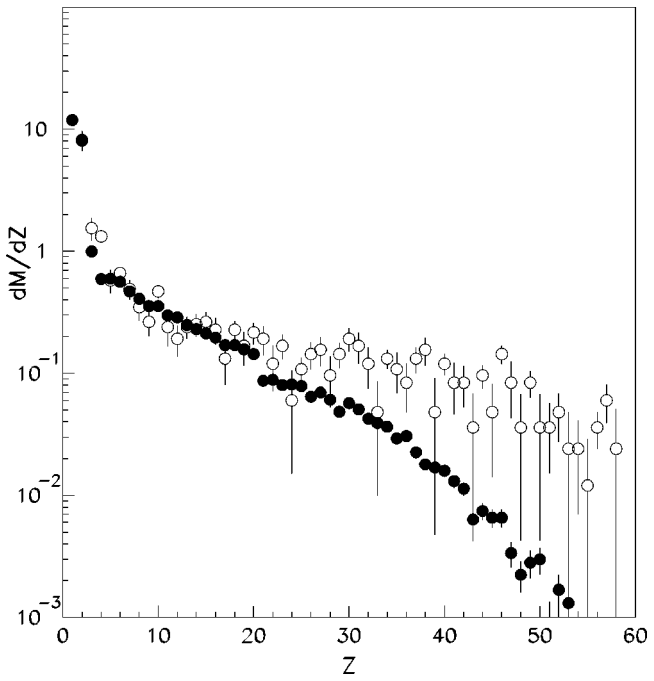

FIG. 6. Comparison between the experimental isotope distribution (solid circles) [12] and the calculated one according to the CoMD model (open circles) for central collisions ($b=0-3.5$ fm) ^{197}Au+^{197}Au at 35 MeV/nucleon. The vertical bars indicate the errors as due to the statistics counting.

shown for the CoMD calculation. The calculations are now in satisfactory agreement with the experimental data. In particular we note that the theoretical prediction of the $Z=2$ yield is about a factor of 10 higher than the QMD case. This is clearly an effect brought by the constraint (15) which favors α particle states. However, the predicted yields of $Z=1$ and $Z=2$ isotopes still show a marked difference with the experimental one.

We have also performed some calculations for the Au+Au system at the same beam energy. Here we are especially interested in central collisions. In fact the behavior of such a small system but so heavily charged is quite puzzling. In Fig. 6 the charge distribution is given for impact parameters up to 3.5 fm and compared to the data [12]. The system was followed for a period of time $t=1500$ fm/c which should be long enough for the system to deliver most of the excitation energy. A few features are worth noticing.

(1) CoMD gives too many protons (not displayed in the figure — out of scale).

(2) The theoretical distribution is slightly shallower than the data. Notice, however, that the data show a jump for $Z=20$, due to the detectors used. If we slightly shift the data yield up for $Z>20$ we get a better agreement with the CoMD results. Therefore we can see from the comparison that the model is working not too bad, especially if one recalls that other dynamical model calculations give very steep distributions.

IV. CONCLUSION

The CoMD model proposed in the present work is able to reproduce with the same set of parameters both the main characteristic of stable nuclei in a wide region of mass ($A=30-208$) and the experimental isotope distribution produced in the collision ^{40}Ca+^{40}Ca and Au+Au at $E_{\rm lab}=35$ MeV/nucleon. This possibility has a considerable relevance because the above-mentioned inclusive information cannot be reproduced by the QMD model. In this respect the success of the CoMD model is due to the constraint represented by the relation (15). This constraint, introduced to describe the fermionic nature of the nuclear many-body problem, affects the dynamics of the nucleus-nucleus collision for two main reasons: (a) the nucleon-nucleon collision rate is higher with respect to the QMD case and (b) the constraint for low-momentum particles produces obviously on the average a nonlocal repulsion effect.

Both these effects play a determining role for the disassembly of highly excited intermediate systems formed at the beginning of a nuclear collision like that investigated in this work. Finally we stress that for the model proposed the typical CPU time needed to follow the time evolution of systems of mass number around 80 for 300 fm/c is quite short: about 10 in a 600 MHz Unix machine.

ACKNOWLEDGMENTS

We thank Dr. K. Hagel and Prof. M. Dagostino for making their data available to us. A.B. thanks Prof. J. Natowitz for discussions and suggestions. T.M. thanks INFN-LNS for warm hospitality during his stay and Dr. M. Colonna for fruitful discussions. Finally M.P. also thanks several experimentalists working at the INFN-LNS for stimulating discussions.

[1] A. Bonasera, F. Gulminelli, and J. Molitoris, Phys. Rep. **243**, 1 (1994).
[2] G. F. Bertsch and S. Das Gupta, Phys. Rep. **160**, 189 (1988).
[3] A. Bonasera, M. Bruno, C. O. Dorso, and P. F. Mastinu, Riv. Nuovo Cimento **23**, 1 (2000).
[4] J. Aichelin, Phys. Rep. **202**, 233 (1991).
[5] H. Feldmeier, Nucl. Phys. **A515**, 147 (1990).
[6] For a review, see H. Feldmeier and Jurgen Schnack, Rev. Mod. Phys. **72**, 655 (2000).
[7] A. Ono, H. Horiuchi, T. Maruyama, and A. Ohnishi, Phys. Rev. Lett. **68**, 2898 (1992).
[8] L. Wilets, E. M. Henley, M. Kraft, and A. D. Mackellar, Nucl. Phys. **A282**, 341 (1977).
[9] C. O. Dorso, S. Duarte, and J. Randrup, Phys. Lett. B **188**, 287 (1987).
[10] T. Maruyama, K. Niita, K. Oyamatsu, T. Maruyama, S. Chiba, and A. Iwamoto, Phys. Rev. C **57**, 655 (1998).
[11] K. Hagel *et al.*, Phys. Rev. C **50**, 2017 (1994).
[12] P. Desequelles *et al.*, Nucl. Phys. **A633**, 547 (1998).